

Consistent proteinaceous organic matter partitioning into mineral and organic soil fractions during pedogenesis in diverse ecosystems

Jinyoung Moon · Kang Xia · Mark A. Williams 

Received: 27 May 2017 / Accepted: 3 November 2018 / Published online: 14 November 2018
© Springer Nature Switzerland AG 2018

Abstract Proteinaceous compounds are critical in soil organic matter (SOM) formation and persistence, but the partitioning into mineral-associated and organic forms during hundreds and thousands of years of pedogenesis are poorly understood across multiple climates and vegetation types. We investigated the partitioning of amino acids (AA) into mineral-bound (MB) and non-mineral associated organic (NMO) soil fractions to discern whether consistent patterns during ecosystem development were observed across two different climates (cool temperate continental, USA; and moist oceanic forests, New Zealand). Although each ecosystem retained unique soil AA signatures, consistent patterns in both systems were observed with three main findings. (1) Regardless of differences in climate and vegetation between the two ecosystems, AA consistently partitioned in similar ways into MB and NMO soil fractions. For example, Thr, Ser, and Asx were relatively more dominant in the NMO

fraction while Arg, Lys, Cys, and Met were relatively more dominant in the MB soil fraction. (2) AA change, showed similar trends related to chemical groupings of positively-charged, polar aromatic, sulfur containing, and non-polar AAs across both ecosystems consistent with changing patterns of soil Fe and Al bearing minerals, such as an increasing weathering index (WI; Fe dithionite/total Fe) and losses of Fe and Al from surface soils during ecosystem development. (3) The pedogenic patterns of AA change, in each system paralleled biological transitions in bacterial communities, suggesting a linkage between the AA sources and the soil sink that contributes to soil organic N. This latter point contrasts with the potential for complete change in soil AA composition that could occur upon processing and binding in soil. Overall, the consistency in the types of AAs that partition into either MB or NMO soil fractions across locations provide evidence of similar processes that contribute to soil organic N accrual across soils. Some AA also appeared to be retained in soil by electrostatic forces, and AA–organic matter interactions, that need further study. Mineral–metal complexation of AAs with sulfur side chain groups, and non-polar interactions, respectively, provide examples of these potential mechanisms for study. The results not only support mechanisms of soil proteinaceous organic matter chemistry being driven by the interactions with the soil matrix, acting as a “sink”, but also draw attention to the sources of organic matter (microbes, plants) in

Responsible Editor: Karsten Kalbitz.

Electronic supplementary material The online version of this article (<https://doi.org/10.1007/s10533-018-0523-1>) contains supplementary material, which is available to authorized users.

J. Moon · K. Xia · M. A. Williams (✉)
School of Plant and Environmental Sciences, Virginia Polytechnic Institute & State University, 312 Latham Hall, 220 Ag Quad Ln., Blacksburg, VA 24061, USA
e-mail: markwill@vt.edu

determining the composition of organic N in soil during pedogenesis.

Keywords Soil organic matter · Microbial · Amino acids · Proteinaceous · Plant · Chronosequence · Mineral

Abbreviations

| | |
|-----|--------------------------------|
| AA | Amino acid |
| SOM | Soil organic matter |
| OM | Organic matter |
| SON | Soil organic nitrogen |
| WI | Weathering index |
| NMO | Non-mineral associated organic |
| MB | Mineral-bound |

Introduction

Proteinaceous compounds are major contributors to soil organic matter accumulation (SOM) and persistence (Zang et al. 2000; Marschner et al. 2008; Knicker 2011; Schmidt et al. 2011; Moon et al. 2016). During SOM formation, some nitrogenous molecules exhibit slow turnover compared to other organic compounds and help to explain, compared to most plant matter inputs to soil, the relatively low C:N ratio of soils (~ 12 – 16) in relatively well developed mineral soils (Knicker 2011). They thus play a key role in determining SOM and carbon (C) turnover and storage (Gårdenäs et al. 2011). More than 90% of soil nitrogen (N) is organic (Stevenson 1982) and the soil organic nitrogen (SON) is predominantly (70–90%) composed of proteinaceous compounds (Leinweber et al. 2013). Proteinaceous compounds including proteins, peptides, and AAs are, thus, quantitatively important and biologically significant molecules associated with both rapidly cycling and persistent SOM.

Molecules have been described as chemically resistant to microbial decomposition in fresh litters (e.g. lignin), but during initial decomposition, organic matter remaining following months to several years may not represent highly recalcitrant organic matter (Hobara et al. 2014; Philben et al. 2016). Though the idea of chemical recalcitrance as playing a major role in persistence of organic matter in soil is debated (e.g. Schmidt et al. 2011), these initial decomposition rates have often been operationally defined as chemically

resistant and extrapolated as long-lived SOM (Meentemeyer 1978) parameterized in C–N models (Parton et al. 1992; Jenkinson and Coleman 2008). However, it is argued that inherently chemically resistant SON structures are not observed in high abundance in most soil ecosystems (Abe and Watanabe 2004), and at best, the proportion of this matter to total SON decreases considerably over several years (Amelung et al. 2008; Grandy and Neff 2008; Dümig et al. 2012). On the other hand, proteinaceous compounds predicted to be labile based on initial litter decomposition are a predominant structure of SON in many natural settings (DiCosty et al. 2003; Abe and Watanabe 2004; Leinweber et al. 2013). Their mean residence time in soil is rather longer than that of some molecules thought to be chemically more resistant (Amelung et al. 2008; Marschner et al. 2008) and their proportion to total SON is often constant or increasing with pedogenesis (Mikutta et al. 2010; Dümig et al. 2012; Moon et al. 2016). These observations suggest that important organo-mineral or organic–organic interactions may play a role in their persistence, perhaps through physicochemical protection (Knicker and Hatcher 1997; Zang et al. 2000; Fan et al. 2004). Describing the distribution of proteinaceous compounds into soil fractions are highly relevant to soil nutrient cycling but also to the broader picture of soil pedogenesis and global biogeochemical cycling.

Determining proteinaceous compounds is often expressed by the distribution of their structural unit, amino acid (Amelung and Zhang 2001; Rovira et al. 2005; Philben et al. 2016). The soil AA distribution changes during soil decomposition of fresh plant residues through microbial activity and turnover. Over periods of several years, which are relatively long in terms of residue breakdown, but relatively short compared to the process of pedogenesis, decomposed litters show relative increases in AAs (Lowe 1973; Rovira et al. 2008; Hobara et al. 2014). Glycine and alanine, which tend to be abundant in bacterial cell walls (Koch 2006); and those of threonine and serine which are abundant in fungal cell wall (Wagner and Mutatkar 1968) increase with litter decomposition. The patterns of AA change during SON transformation agrees with other indicators, such as amino sugars, diaminopimelic acid and the D-form of some AAs, which are common in microbial cell walls (Amelung 2003) and tend to accumulate in soil during litter decomposition (Hobara et al. 2014; Philben et al.

2016). However, less is known about the occurrence of AAs as they are fractionated and partitioned into mineral and non-litter organic matter, nor their potential for change over longer pedogenic scales, whereby other interactions such as mineral and organic binding play a role.

A large portion of SOM associated with mineral particles is identified as proteinaceous (Knicker and Hatcher 1997). Their essential roles as structural bridges between mineral surface and other SOMs are described in organo-mineral complexation, onion layering (Sollins et al. 2006) and micellar coating models (Kleber et al. 2007). Studies on the relative distribution of AA associated with mineral particles reveal that chemically-driven interactions such as electrostatic attraction may influence selective accumulation of certain AAs. Positive and negatively charged AAs in short term (several days) batch equilibrium studies tended to be retained in accordance with the cation and anion exchange properties of soil (Vieublé Gonod et al. 2006; Strahm and Harrison 2008). Furthermore, studies using soil chronosequences show that mineral associated AA distribution changes with pedogenic shifts in soil properties (e.g. CEC, pH,) during the processes of weathering and long-term SOM change (Mikutta et al. 2010; Moon et al. 2016). Further investigation across ecosystems is needed to better understand the fate of proteinaceous compounds and develop models of proteinaceous-mineral and -organic interactions during pedogenesis.

Whether the fractionation of proteinaceous compounds between mineral and organic phases and their patterns of change during pedogenesis share consistent trends across ecosystems with different climates and vegetation communities is an open question. In this study, two major questions were asked. (1) Are there patterns of AA association into mineral and organic matter fractions in two climatically different ecosystems? And (2) are there patterns during soil development related to biological and pedogenic changes in soil? We thus examined the relative distributions of AA in soil fractions in soil chronosequences aged hundreds to thousands of years under two different climates: cool temperate continental at WSP (MI, USA) and moist oceanic (Haast, NZ) rainforest. It was hypothesized that there would be differential AA fractionation to mineral bound (MB) and non mineral organic (NMO) phases, that these MB and NMO fractionations would, respectively, show similarities

across locations, and that change in AAs would follow similar patterns of change during pedogenesis, especially in the mineral fraction, related to electrostatic charges.

Methods and Materials

Site descriptions

This study utilized chronosequences to understand chemical, biological, and physical changes that occur in soil ecosystems as a consequence of pedogenesis. Information on the mineralogy of both locations are not available across most soil ages, and so a summary table is provided describing the general Fe and Al bearing minerals of the soils (Tables 1, 2). Information related to indications of chemical change in both systems are further described below.

Lake Michigan Chronosequence, U.S.A.
(Michigan site; Wilderness State Park, WSP)

Location and climate

The Michigan site consists of a series of beach-dune ridges bordering Lake Michigan (N 45.72729, W84.94076). There are > 108 eolian deposited dune ridges running parallel to the shoreline with depositional ages from present day to ~ 5 k years (Lichter 1995b). The site was located at the interface of a temperate and boreal climate region. Temperature and precipitation average 6.3 °C and 77.2 cm per year, respectively.

Parent materials and soil types

The dune ridges have a parent material originating from glacial deposits and Paleozoic bedrock underlying the basin of Lake Michigan. The parent material and dune formation processes are thought to be similar across the dune sequence (Lichter 1995b). Fine sands deposited on the lake shore are dominated by quartz but contain numerous other minerals in minor quantities (Lichter 1995a). The youngest soils (< 185 years) are mapped as dunes which then develop into Deer Park sands (soil series) and described taxonomically as mixed, frigid, Spodic Udipsamments. The oldest soils (> 1475 years) tend

Table 1 Iron and aluminum-fractions at Wilderness State Park, MI, USA

| Age (ky) | Fe (t) Total | Fe(d)/Fe(t) W- Index | Fe(d) Crystalline | Fe(o) Amorphous | Al(t) Total | Al(d) Crystalline | Al (o) Amorphous |
|----------|-----------------|-------------------------|----------------------|--------------------|----------------|----------------------|---------------------|
| 0.11 | 1.96 a | 0.49 a | 0.80 a | 0.25 a | 0.98 a | 0.05 a | 0.04 a |
| 0.15 | 1.83 a | 0.59 b | 1.09 b | 0.32 b | 0.99 a | 0.11 a | 0.09 a |
| 0.21 | 1.82 a | 0.72 c | 1.30 c | 0.46 c | 0.94 a | 0.24 ab | 0.19 b |
| 0.45 | 1.57 b | 0.94 d | 1.46 c | 0.51 c | 0.99 a | 0.36 b | 0.29 c |
| 0.85 | 1.14 c | 0.88 d | 0.95 d | 0.22 a | 0.74 b | 0.20 ab | 0.23 b |
| 1.5 | 0.82 d | 0.63 b | 0.45 d | 0.10 d | 0.64 c | 0.11 a | 0.16 b |
| 2.4 | 0.87 d | 0.75 c | 0.52 d | 0.17 ad | 0.63 c | 0.19 ab | 0.19 b |
| 3.2 | 0.69 e | 0.95 d | 0.62 d | 0.20 a | 0.51 d | 0.15 a | 0.15 b |
| 4.0 | 0.57 e | 1.06 e | 0.58 d | 0.19 a | 0.45 e | 0.21 ab | 0.21 b |
| r value | – 0.91* | 0.64* | – 0.69* | – 0.57* | – 0.94* | 0.24 | 0.38* |
| Slope | – 0.33 | 0.08 | – 0.17 | – 0.05 | – 0.14 | 0.05 | 0.02 |

Except for the weathering ratio (W-Index), units in mg g^{-1} soil

Different letters indicate statistical differences within a column ($p < 0.05$). Asterisks across rows are indicative of statistically significant correlations associated with change in ecosystem age ($p < 0.05$)

Table 2 Iron and aluminum-fractions at Haast

| Age (ky) | Fe(t) Total | Fe(d)/Fe (t) W-index | Fe(d) Crystalline | Fe(o) Amorphous | Al(t) Total | Al(d) Crystalline | Al(o) Amorphous |
|----------|----------------|-------------------------|----------------------|--------------------|----------------|----------------------|--------------------|
| 0.18 | 21.0 a | 0.15 a | 3.25 a | 2.2 a | 3.80 a | 0.067 a | 0.053 a |
| 0.39 | 17.6 b | 0.19 b | 3.23 a | 2.1 a | 3.70 a | 0.15 a | 0.063 a |
| 0.52 | 15.4 b | 0.21 b | 3.23 a | 2.1 a | 3.50 b | 0.17 a | 0.05 a |
| 1.8 | 13.1 c | 0.14 a | 1.9 b | 0.65 b | 4.20 c | 0.45 b | 1.07 b |
| 4.4 | 10.7 d | 0.13 a | 1.4 b | 1.2 b | 2.80 d | 0.57 b | 1.17 b |
| 6.5 | 8.30 e | 0.28 c | 2.35 b | 1.7 ab | 2.21 e | 1.39 c | 1.41 b |
| r value | – 0.80* | 0.45* | – 0.68* | – 0.38 | – 0.87* | 0.78* | 0.89* |
| Slope | – 1.51 | 0.01 | – 0.20 | – 0.09 | – 0.24 | 0.15 | 0.22 |

Except for the weathering ratio (W-index), units in mg g^{-1} soil

Different letters indicate statistical differences within a column ($p < 0.05$). Asterisks across rows are indicative of statistically significant correlations associated with change in ecosystem age ($p < 0.05$)

to be mapped to the Roscommon series, and are mixed, frigid Mollic Psammaquents. The changes in soil types suggest the process of chemical weathering of minerals and organic matter change are consistent with pedogenic theory (Buol et al. 2011).

Vegetation

Dune-building grass species (mostly *Schizachyrium scoparium*) are replaced by evergreen shrubs (mostly family Ericaceae) and short statured trees (e.g.

Juniperus) at around 210 years and these are then replaced by Juniper and then mixed pine dominated forests between 450 and 845 years (Williams et al. 2013). The pine forests consisted mostly of members of the family Pinaceae, including *Pinus strobus* and *Abies balsamea*. Once the forest matured further, *Pinus resinosa* increased while *Juniperus* became rare, and usually absent. Except for increasing cover of *Betula* and *Quercus* sp (~ 5 –10% cover), the plant species composition stabilized at ~ 845 years and there was no major change in the overstory plant

community structure during late ecosystem development.

Bacterial community

The chronosequence gradient showed a number of changes in phyla but were generally dominated by the abundance and dynamics of Acidobacteria, Actinobacteria, and Alphaproteobacteria, comprising 71% of all the sampled sequences (Williams et al. 2013). Other less abundant phyla (< 4%) were Bacteroidetes, Cyanobacteria, Firmicutes, Planctomycetes, Betaproteobacteria, and Gammaproteobacteria. Between early (< 450 years) and late (> 450 years) ecosystem development, Acidobacteria increased approximately 6-fold from around 4% to ~ 30%. Actinobacterial abundance declined, in contrast, from around 60 to ~ 35% during this same time. The gradient of ecosystem development also was described by changes in low abundance taxa, with Bacteroidetes and Firmicutes, for example declining and Planctomycetes and Gammaproteobacteria increasing 4-fold. Cyanobacterial abundance declined from 5% to less than 0.5% following 210 years of ecosystem development.

Haast River Chronosequence, New Zealand (Haast site)

Location and climate

The Haast site consists of a set of shore-parallel coastal dunes (beach ridges) on a prograding coastal plain west of the Southern Alps, northwest of the Haast River, on the west coast of the South Island of New Zealand (43°43'20"S, 169°4'30"E) (Eger et al. 2011). The site is under lowland temperate rain forest. Temperature and precipitation varies less through an annual cycle compared to WSP, averaging 11.3 °C and 346 cm per year, respectively. Relative humidity averages 83%.

Parent materials and soil types

To the north and south of the dune sequence are large alluvial fans of the Waita and Haast Rivers, respectively (Rattenbury et al. 2010). Parent material is uniform quartzo-feldspathic dune sand derived from well-foliated schist. The mineralogy of the

unweathered sand appears relatively uniform across the chronosequence, being 40–50% quartz, with the remainder feldspar, mica and chlorite (Palmer et al. 1985). Short lived phases of Entisols followed by Inceptisols culminate in the formation of persistent Spodosol forms within 1 k to > 30 ky depending on rainfall. Soils develop rapidly to podzols (Spodosols) under the super-humid climate of the west coast of New Zealand. Eluvial horizons are reflected by low pH (< 4.5) in the upper part of the soil and illuvial horizons by accumulation of poorly or noncrystalline Fe, Al and occasional Si together with organic matter. These trends are accompanied by decreasing base saturation, increasing C/N ratios, and depletion of alkaline cations and apatite phosphorus. Impeded drainage is typical of more advanced stages of Spodosol pedogenesis and decline of coarser fractions to form cemented iron pans or B_s horizons as a result of iron translocation (Eger et al. 2011). These patterns of soil change thus support pedogenic theory via processes of mineral weathering and horizonation.

Vegetation

Forests in the region are mixed conifer–broadleaf temperate rain forest (Turner et al. 2012). The conifers consist of members of the family Podocarpaceae, including *Dacrydium cupressinum*, *Prumnopitys ferruginea*, *Podocarpus cunninghamii*, and *Phyllocladus alpinus*. And the tree fern species (*Dicksonia squarrosa* and *Cyathea smithii*) were observed in the conifer forest. The conifers and tree ferns decrease and replaced by woody angiosperms in the 1826 years old soil and older. The woody angiosperms in the area include mainly *Weinmannia racemosa* and *Lophozonia menziesii*.

Bacterial community

Bacterial communities showed patterns of change during pedogenesis, similar to those at WSP, with the largest change during the first several hundred years after dune stabilization (Jangid et al. 2013). The most abundant bacterial taxa were Alphaproteobacteria, Actinobacteria and Acidobacteria. The Bacteroidetes, Actinobacteria, Cyanobacteria, Firmicutes, and Betaproteobacteria all showed a general decline in abundance as pedogenesis proceeded, while Acidobacteria, Alphaproteobacteria, and Planctomycetes

tended to increase as soils aged. Bacterial communities changed in ways that appear to be consistent with a model of ecosystem progression and retrogression.

Soil sampling

Michigan site (Wilderness State Park)

Five replicates of top soil samples were collected from the incipient A-E horizon (0–15 cm depth, 5 cm dia.) in nine dunes of age 105, 155, 210, 450, 845, 1475, 2385, 3210, and 4010 years at the Michigan site by the same way as previous published literature (Williams et al. 2013). Each replicate was separated by 10 m intervals across transects along each dune's crest. Thus, 45 plots were sampled. The soil samples were stored in sterile Whirlpak bags, and frozen in coolers with dry ice and kept at $-20\text{ }^{\circ}\text{C}$ until processing.

Haast site

Four replicates of top soil samples were collected from mineral soil layer (0–20 cm depth, 2.5 cm dia.) in six dunes of age 181, 392, 517, 1826, 4422, and 6500 years at the Haast site by the same manner as previous published literature (Jangid et al. 2013). Each replicate plot was separated by ~ 50 m intervals along the crest of each dune and ten locations within each plot were chosen to obtain a representative and well mixed soil. Thus, 24 plots were sampled. The soil sample bags were frozen and immediately placed in a cooler packed with dry ice. Upon arrival in the laboratory, soils were thawed for ~ 30 min, homogenized through a 2-mm sieve, extraneous roots and NMO materials were removed, and the samples were kept at $-20\text{ }^{\circ}\text{C}$ until processing.

Both soils were sampled to assess the surface A-B and A-E horizons that make for the best comparison across locations. Given the complexity of the soil forming process, it must be recognized that the simultaneous sampling the A and E/B horizons to a different extent across soil ages adds variability and could affect interpretation of the results. This sampling could, for example, affect relationships between crystalline and amorphous Fe fractions. Because the WSP soils are younger, contain fewer “easily” weatherable minerals, and a cooler climate, the rates of weathering also differ from those of Haast. The sampling, however, was conducted to make this

comparison as clean as possible and compare the soil zones of the surface A which accrue organics but also leach to form regions of translocated minerals.

Hydrolysable AA analysis

The hydrolysable AAs in the whole and mineral soil were acid digested, purified, derivatized, and then analyzed by high performance liquid chromatography (HPLC) derivatization, following the procedures from Moon et al. (2016). Briefly, collected soil was hydrolyzed in 6 M HCl with an internal standard (L-norvaline) at $110\text{ }^{\circ}\text{C}$ for 24 h (Amelung and Zhang 2001). The soil hydrolysates were centrifuged. The supernatant was diluted in ultra-pure water to achieve pH 1.37 and cleaned on a preconditioned Dowex 50W X8 resin. The interfering metals were removed by rinsing with 0.1 M oxalic acid (pH 1.6–1.7). AAs retained on the resin were eluted with 3 M NH_4OH , filtered through a $0.22\text{ }\mu\text{m}$ polyvinylidene fluoride membrane syringe filter, vacuum-dried, reconstituted in 0.05 M HCl, and finally derivatized using the AccQ FluorTM reagent kit (Waters Co. Cat# WAT052880) following the standard protocol from Bosch et al. (2006) and Hou et al. (2009). Chromatographic separation on the HPLC 1260 Infinity system (Agilent Technologies, USA) was carried out on a reversed phase column (Waters X-Terra MS C18, $3.5\text{ }\mu\text{m}$, 2.1150 mm), following the instrument setup from Moon et al. (2016). Hydrolysable AAs in the samples were qualified and quantified by comparison with AA standard solutions. The detection limits, recovery, and precision of determination of each AA derivatives were reported in Ma (2015). Each AA standard solution contained 20 AAs including alanine (Ala), arginine (Arg), aspartic acid (Asp), asparagine (Asn), cystine (Cys–Cys; more stable form in oxidative condition than monomer cysteine), glutamic acid (Glu), glutamine (Gln), glycine (Gly), histidine (His), isoleucine (Ile), leucine (Leu), lysine (Lys), methionine (Met), phenylalanine (Phe), proline (Pro), serine (Ser), threonine (Thr), tyrosine (Tyr), tryptophane (Trp), and valine (Val). During acid hydrolysis, Trp is often destroyed, Asn and Gln were transformed to Asp and Glu, respectively. The combined peak of Asp and Asn was denoted as Asx (Asp + Asn) and the combined peak of Gln and Glu was denoted as Glx (Gln + Glu). A total of 17 AA peaks were quantified for hydrolysable proteinogenic AAs.

Soil C fractionation and associated AA analysis

Following fractionation, mass of the total soil, light, and heavy fractions were determined and C contents measured. The heavy fraction was isolated by the density method, followed by AA analysis (Moon et al. 2016). Air-dried soils were fractionated using sodium metatungstate (SMT, $\text{H}_2\text{Na}_6\text{O}_{40}\text{W}_{12}$) solutions with a density of 1.65 g cm^{-3} . The mixture was vigorously agitated on a shaker until the soil was completely dispersed; and was then centrifuged. The floating particulate matter (light fraction) containing no identifiable plant pieces was carefully separated from the heavy fraction. The dried heavy fraction was weighed and hydrolyzed using the analysis as described above. The AA released from the SMT-isolated heavy fraction was interpreted as the mineral bound (MB) AA fraction. The non-mineral associated organic (NMO) fraction of AA was interpreted by subtracting MB AA from those of the whole soil amino acids.

Total soil Fe and Al was extracted using a mixture of HNO and HClO acids (Lichter 1998). The amount of Fe (Fe(o)) and Al (Al(o)) in poorly crystalline, hydrous oxides was measured by acid-oxalate extractions on whole soils. Dithionite-citrate extraction of Fe (Fe(d)) gives an estimate of primarily crystalline phases, but may include some secondary amorphous oxides (Jaworska et al. 2016). A weathering index (WI; $\text{Fe(d)}/\text{Fe(t)}$) for Al and Fe was also calculated. Extractions were analyzed in solution using an ICP-MS.

Statistical analysis

For univariate analysis, WI, Al and Fe fractions (total, crystalline, and amorphous) and NMO and MB fractions were compared across ages using ANOVA. Regression analysis was used to assess correlations between soil age and change in elemental fractions with ecosystem development. In a few cases, when multivariate analysis were not appropriate, changes in AA and AA groups with age were also tested ($p < 0.05$).

Multivariate statistics were involved in the bulk of the statistical tests. For these comparisons, molecular species of AA abundance were transformed using general relativization to remove the influence of absolute abundance on ordination. Multi-Response Permutation Procedures (MRPP), Sorenson distance

matrix, and Nonmetric Multidimensional Scaling (NMS) ordination were performed using the PC-ORD software version 6.0 (MjM Software, Gleneden Beach, OR, USA) to compare the effects of site and soil age on the relative abundance of 17 proteinogenic AAs in MB and NMO. A Sorenson distance measure was used because it ignores the joint absences and retains sensitivity in heterogeneous data sets without excessive sensitivity to outliers. A Sorenson distance measure was also applied to each domain separately. The observed AA dataset was analyzed separately from that of the predicted bacterial proteome AA dataset (Chen et al. 2013). The metrics for the absolute values of the Sorenson distance index were then used. The cutoff of statistical significance for multivariate statistical methods was $p < 0.01$.

Linear, quadratic, and cubic polynomial regressions were tested and those with the best fit were used for presentation and statistical testing of the different chemical AA groupings during soil development. Normality tests of AAs were first confirmed using SigmaPlot version 11.0 (Systat Software, San José, CA, USA). Plots of mol% AA with soil age were tested for significantly different patterns of relative change ($p < 0.05$) with age, separately for each location. A comparison of the relative change between both locations was used to test whether each location followed a similar pattern of change ($p < 0.05$).

Results

Physicochemical properties of soils and AA associated with MB and NMO soil

Recoveries of heavy and light fraction remained above 79%, averaging 92.6 and 95.6% in the WSP and Haast samples (Supplementary Table A1). In WSP, the light fraction increased during the first 210 years of ecosystem development, but then reached a steady state. The amount of carbon (C) in the light fraction ranged from being similar but sometimes up to 7X more than the heavy fraction. The amount of C in Haast fractions average $\sim 6\text{X}$ more than at WSP, with the light containing similar amounts of carbon than the heavy fraction. There was not a clear trend with ecosystem development, however, total C values increased ($p < 0.05$; $r > 0.28$) from the single youngest age to all latter ages. Overall these results are

supported by AA abundances, whereby $\sim 210 \mu\text{g g}^{-1}$ soil were derived, on average, from the MB and $\sim 860 \mu\text{g g}^{-1}$ soil from the NMO at WSP. Similarly, the amounts of AA in Haast were $950 \mu\text{g g}^{-1}$ and $4800 \mu\text{g g}^{-1}$ soil derived from the MB and NMO fractions, respectively. In general, hydrolysable AA averaged around 6–10% of C (up to 18% of N) in each fraction.

Mass of C in light fractions per mass of each respective fraction (mg C g^{-1} fraction) averaged 20–25% for both soils. In contrast, the mass of C per mass in the heavy fraction averaged around 2.5% for WSP and 7–25% for Haast, however, there were no significant trends associated with age. The percentage of mass in the light, but not the heavy fraction increased linearly with age ($r > 0.23$; < 0.05). This latter result indicates a tendency for C to accrue more in the light than the heavy fraction.

Total soil Fe and Al and their crystalline and amorphous fractions changed similarly, both negatively and positively, during ecosystem development in both chronosequences (Tables 1, 2), indicating similar patterns of soil Al and Fe bearing mineral change during ecosystem development. Many of these mineral changes were well correlated with AA change with soil development (Table 3). One difference between locations was a result of the changes that

occur at Haast, the older chronosequence, where both fraction and AA changes converge from previous trends at 6500 years. This change was attributed to the greater degree of weathering. Concentration of these fractions, however, were 2–6X greater in Haast than WSP. Both soils showed distinct declines in the amorphous (o) Fe soil pools, but increases in Al bearing mineral fractions during ecosystem development. There is a general loss of total soil Fe and Al, an indication of weathering from the surface soils. Another primary indicator of weathering activity is the WI, which increased as expected as the soils aged. An increasing WI ratio reflects the progressive weathering of Fe bearing minerals with time (Jaworska et al. 2016). Dithionite extractable Al, it should be noted, does not necessarily reflect only crystalline Al phases and therefore, though we report the results, do not interpret them. The main point of focus, however, was that changes in total and operationally defined Al and Fe pools are indicative of the process of pedogenesis and help to explain changes in AA pools during ecosystem development.

Overall, the AA amounts were derived from non-living plant and microbial sources, where microbial biomass would account for less than 5% of the expected AAs (Moon 2015). Thus, the mol% and dynamics of AAs will be interpreted through the lens

Table 3 Numerous correlations between changes in fractions of metal bearing minerals and AA groupings at both Haast and WSP

| | Fe crystalline | Fe amorphous | Total Fe | Total Al | Al crystalline | Al amorphous |
|----------------|----------------|---------------|---------------|---------------|----------------|---------------|
| WSP | | | | | | |
| Positive AA | – 0.44 | – 0.42 | – 0.85 | – 0.73 | 0.15 | 0.70 |
| Negative AA | 0.50 | 0.45 | 0.54 | 0.54 | 0.09 | – 0.06 |
| W-index | 0.01 | 0.06 | – 0.62 | – 0.58 | 0.44 | 0.76 |
| Polar-aromatic | – 0.34 | – 0.26 | – 0.52 | – 0.59 | 0.18 | 0.21 |
| Non-polar | 0.57 | 0.46 | 0.91 | 0.87 | – 0.26 | – 0.47 |
| Haast | | | | | | |
| Positive AA | – 0.13 | – 0.76 | – 0.19 | 0.30 | – 0.33 | 0.31 |
| Negative AA | – 0.47 | 0.30 | 0.28 | – 0.15 | 0.60 | 0.01 |
| W-index | 0.26 | 0.39 | – 0.40 | – 0.61 | 0.53 | 0.15 |
| Polar-aromatic | – 0.28 | – 0.92 | – 0.36 | 0.27 | – 0.24 | 0.49 |
| Non-polar | – 0.19 | 0.68 | 0.78 | 0.22 | 0.01 | – 0.60 |

Numbers that are bolded show statistically significant changes ($p < 0.01$) that occur in similar patterns at both Haast and WSP. Change in total Fe, W-index, and Polar-aromatic AA had the most numerous correlations shared between sites. The W-index is thought to be the best descriptor of pedogenesis because it integrates the ratio of crystalline to total elemental Fe as an indicator of weathering (Jaworska et al. 2016)

of non-living organic matter. The relative distributions of MB AA compared to NMO were highly consistent in both sites. Gly, Ala and Ser, for example, dominated NMO compared to MB soil AA abundance at each location. Eleven out of seventeen AAs were shown to have common trends, either being relatively enriched or depleted in the MB compared to NMO fractions (Fig. 1). The common enriched AAs of the MB hydrolysates compared to the NMO hydrolysates were (1) positively charged AA (His, Lys, and Arg) and (2) AAs containing aromatic and hydroxyl side chain group (Tyr and His), and (3) sulfur group AAs (Met and Cys). Negatively charged AAs (Asx) and those with neutral polar groups (Ser and Thr), were less enriched in the MB compared to the NMO. The common trends in AAs across sites could thus be related to differences in the chemical properties of AAs (Fig. 2) and soil properties. Though not a comparison between MB and NMO fractions, Table 1 and 2 provide an example of how whole-soil Fe and Al bearing minerals could differ from that of NMO fractions. The average pI, at both locations furthermore, was greater in the MB than those in NMO at

both sites (Fig. 3), indicating a tendency toward more positively charged AAs. The chemistry of AAs in MB relative to NMO associations can help to explain some of the differences in AA distribution, however other changes related to aromatic, polar groups, and sulfur need further investigation.

Site and age-related variations in mineral soil AA distribution

Site specific properties were a strong factor for shaping both NMO ($A = 0.26$, $p < 0.001$ from MRPP; Fig. 4) and MB soil AA distribution (Table A2). In this NMS bi-plot, the AA distributions were clustered by sites on Axis 1 which explained a large portion (57%) of the total variance. The site-specific AA patterns were largely driven by mol% differences in Gly (greater in Haast site) and to a lesser extent Arg, Phe, Leu, and Ile (greater in Michigan site).

Age-related AA patterns within each site were mainly correlated with Axis 2, which explained about 28% of the variance, and were described by patterns associated with ecosystem development, however,

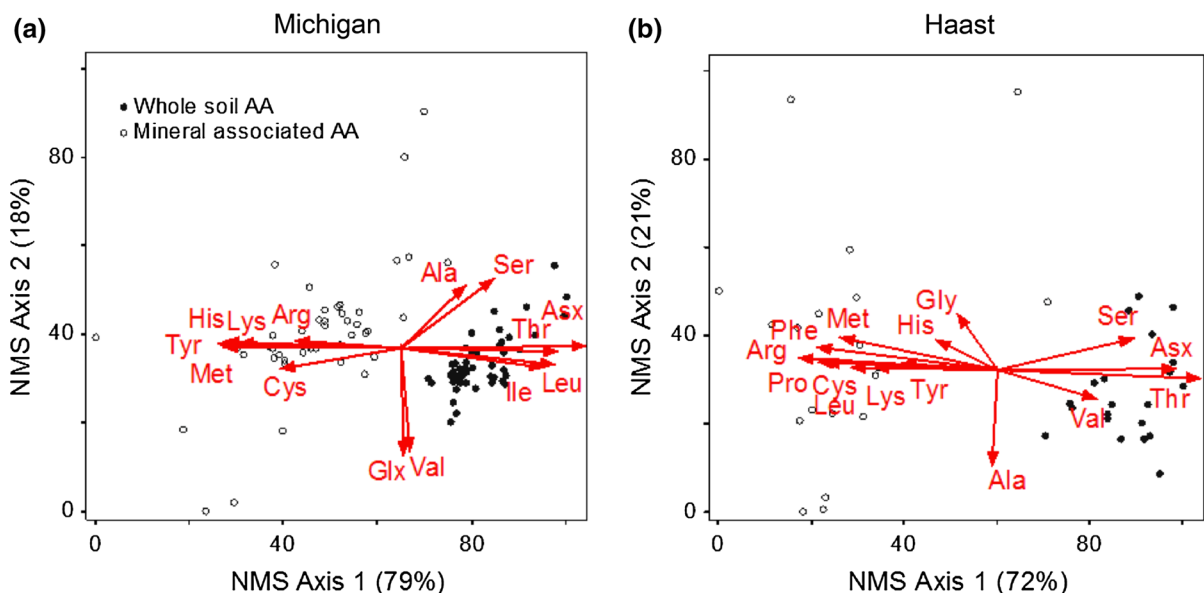


Fig. 1 Comparison of the mol% AA distribution showing how the two chronosequence soils, Michigan (a) and Haast (b), share similar amino acid fractionation into mineral bound (MB) relative to that of non-mineral organic (NMO) soil. Despite geographic, climatic, and parent material differences, amino acids tend to associate in one fraction or the other. The results reflect nonmetric multidimensional scaling (NMS) to

graphically describe the differences. Each axis represents a new dimension that reflects most of variation across the 17 amino acids. The AA vectors describe the direction and strength of the relationship between individual AAs and ordination scores; showing only vectors with an $r^2 = 0.3$. The final stresses were 8 and 11 for (a, b). Percentage on each axis denotes the amount of variability associated with each axis

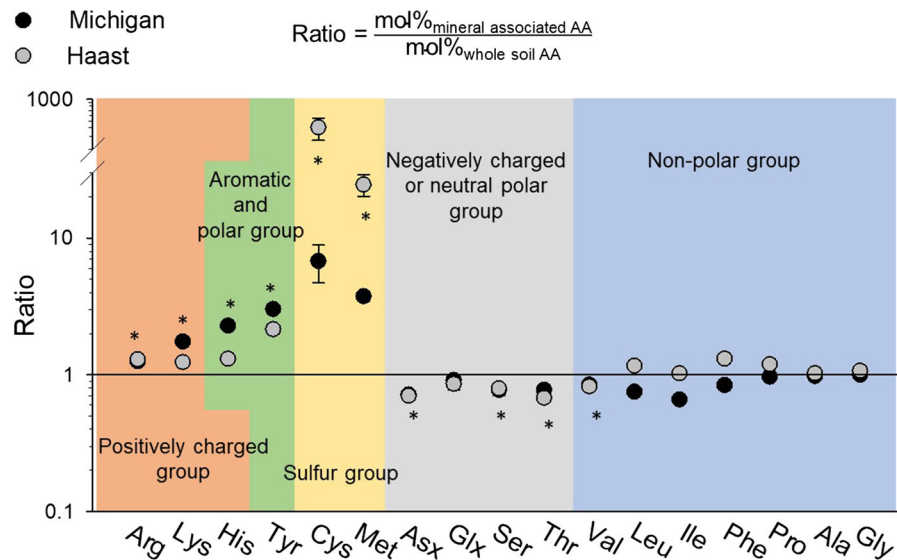
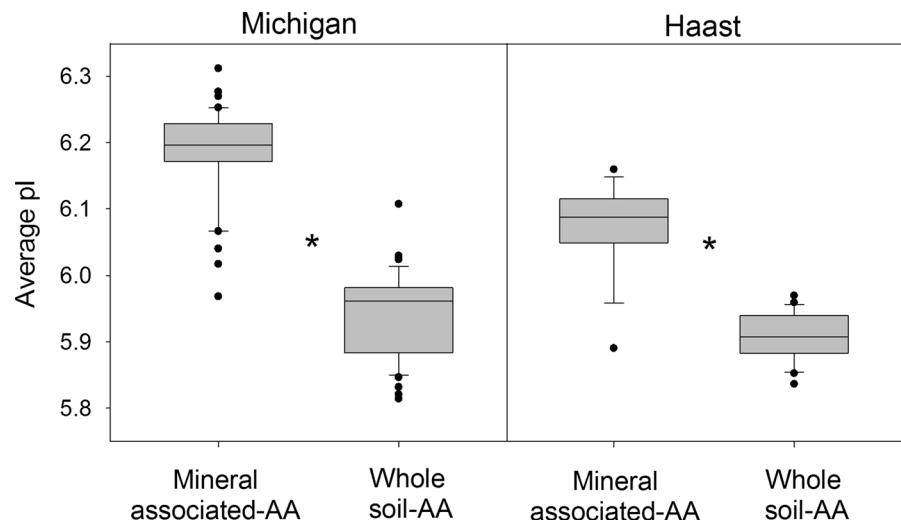


Fig. 2 Relative mol% differences in MB compared to NMO soil amino acids (x-axis) showing how the chemical differences in amino acid types (separated by color and text description) are consistent across both soil chronosequences. The consistent changes between mineral and whole-soil fractions were related to sulfur, aromatic, polar and positively charged groups. Ratios of each amino acid (y-axis) were calculated by dividing the

mol% of mineral compared to whole soil amino acids. A ratio higher than one is indicative of enrichment, while a ratio value lower than one indicates depletion of amino acid on the mineral associated compared to the whole soil OM hydrolysate. “*” indicates that the ratios for both chronosequence soils shared statistically significant differences ($p < 0.05$) from 1. (Color figure online)

Fig. 3 The average pI for both Michigan (left) and Haast (right) soils describing the greater net positive charge of amino acids in mineral associated compared to whole soil fractions. The Box plot shows the minimum, first quartile, median, third quartile, and maximum values of the raw data. *Statistical differences, $p < 0.05$



there were different types of change dependent on location (Fig. 4). Amino acids within the mineral fraction tended to change less than those describing the NMO soil fraction with age. Amino acid change with pedogenesis was thus most strongly related to the NMO-dominated fraction rather than that of the MB.

When analyzed separately to remove the overriding effect of location, several similar patterns of AA change with age were observed in the NMO soil fraction. In both sites, patterns of AA change with age were described (MRPP $A = 0.36$, $p < 0.0001$ in Michigan and $A = 0.27$, $p < 0.0001$ in Haast) in the NMO but not the MB fraction (Supplementary

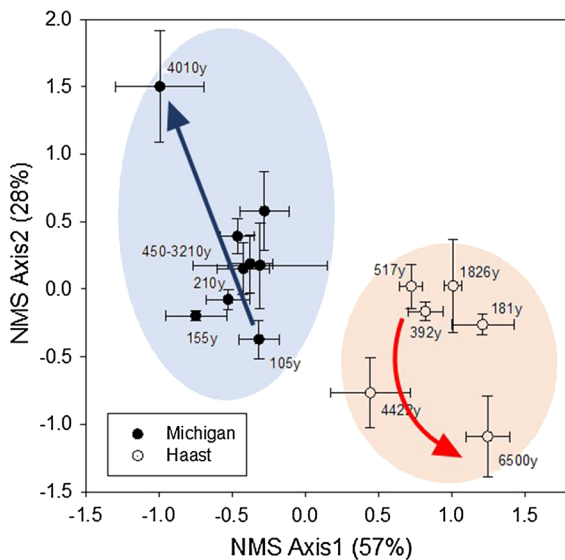


Fig. 4 Nonmetric multidimensional scaling (NMS) ordination highlighting the generally distinct changes in amino acids between the two chronosequences, and patterns of change with soil age, from Michigan (black circle) and Haast (dot circle). Each axis represents a new dimension that reflects most of the variation across the 17 amino acids. Error bars in black and dot circle represent standard error ($n = 5$ for Michigan and $n = 4$ for Haast). The final stress for black and dot circle were both 17. Percentage on each axis denotes the amount of variability associated with the axis

Table A2). It is notable that patterns of change in AA were best viewed when grouped into chemically similar categories, rather than individual AA (Fig. 5). Linear and non-linear patterns were tested for best fit using hyperbolic regression (polynomial quadratic: $f = y_0 + a*x + b*x^2$ and cubic: $f = y_0 + a*x + b*x^2 + c*x^3$) to describe the change in mol% of each AA group with age (Fig. 5). The independent chronosequences were often similarly described by patterns of change with pedogenesis, but it is also worth noting that the Haast ecosystem age was up to several thousand years more than that of Michigan and has a greater climate driven rate of weathering that helps to explain additional chemical change that could not be observed at Michigan. Both sites were described by increasing levels of positively charged AAs with age, however, there appeared to be a decline in positively charged AAs at the oldest soil of the Haast chronosequence. These results were mirrored by a decrease in negatively charged AAs in WSP, and the tendency for greater negatively charged AA in Haast. Polar aromatic, sulfur containing, and non-polar AAs, also tended to show similar trends

with age at both locations, though the polar aromatic group appeared to decline in the oldest soil of the Haast chronosequence. Overall, when grouped into chemical categories there were many similar patterns with age in both sites, up to around ~ 4500 years, but with a few different shifts in the Haast chronosequence as the soil reached 6500 years post-deposition of parent material.

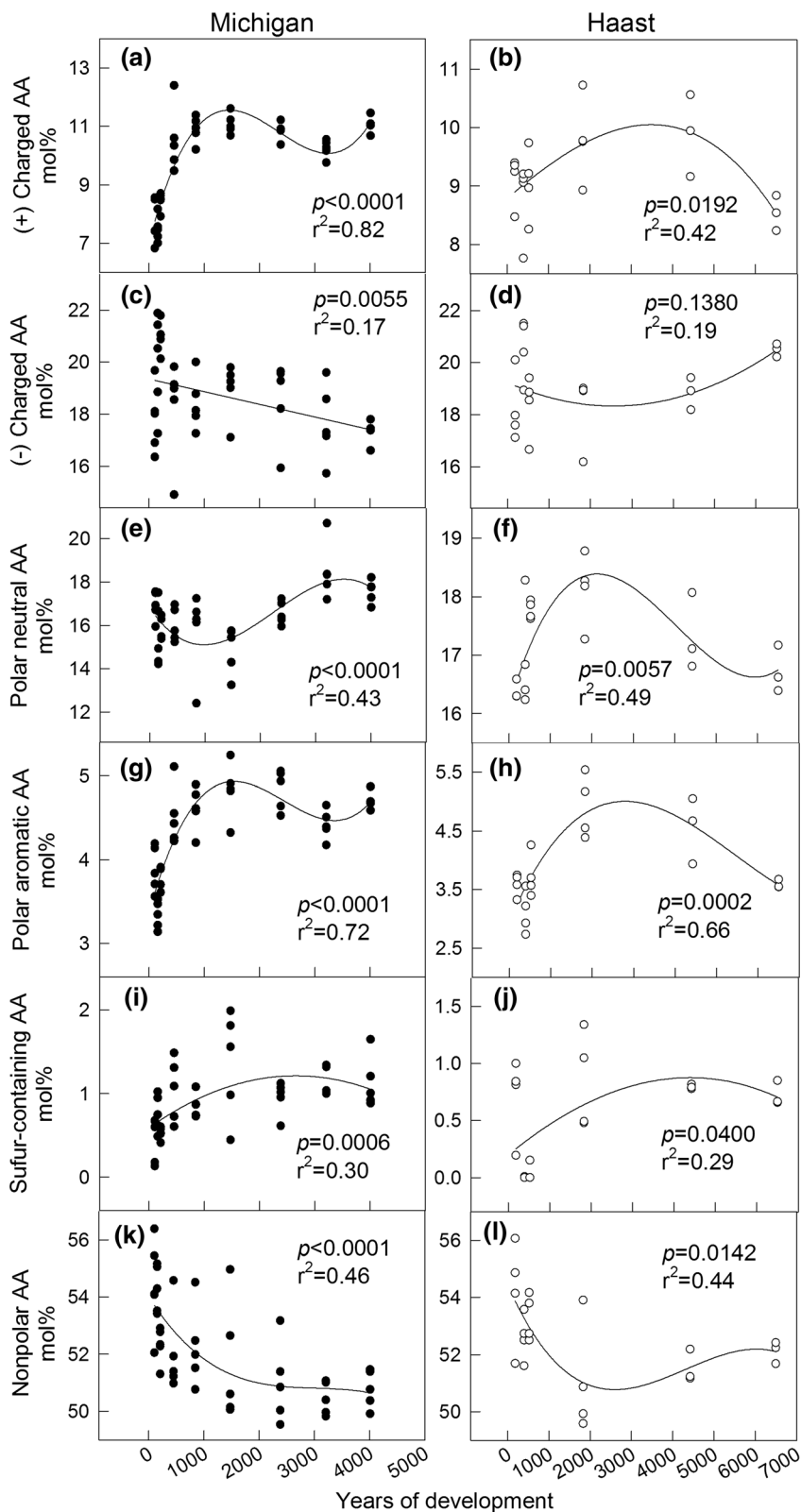
Pedogenic pattern of whole (NMO and MB) soil AA distribution and bacterial communities

The overall pedogenic patterns of NMO soil AA distribution mimicked the successional patterns of bacterial community composition with site age (Fig. A1). The Sorenson distance from the earliest age of each site (105 years on Michigan site and 181 years on Haast site) was used as the baseline to assess the degree of AA change with that of bacterial community composition. Bacterial community composition was a strong predictor of soil AAs ($r^2 = 0.58$, $p < 0.0001$; Fig. A2), especially until about 1500 years, and to a lesser extent the predicted bacterial proteome ($r^2 = 0.22$, $p < 0.0001$; Fig. A3). Before about 1500 years, both AA distribution and bacterial community composition changed dynamically. After about 1500 years, on the other hand, bacterial community composition did not change while AA profiles, did sometimes change. It is also notable that a strong relationship was observed between AA chemical groups, such as positive and polar, with that of changing bacterial communities (Supplementary Table A3). This comparison thus provided evidence that a consistent relationship existed between soil AA patterns and bacterial community composition over pedogenic times scales in independent chronosequences of contrasting climates. Figures A4–A5 show relationships between soil bacterial communities and that of plants, and that plants are not good predictors of soil AAs during ecosystem development. Amino acids within the mineral fraction tended to change less than those describing the NMO fraction with age (Fig. A6).

Discussion

The results supported the hypothesis that proteinaceous AA would partition differently between MB and

Fig. 5 Best fit regression, including linear and polynomial, showing numerous patterns (increasing, decreasing) of change (e.g. increasing, decreasing) in amino acid chemical groups, extracted from NMO soil, and their change with soil depositional age (x-axis) in Michigan (left) and Haast (right) soils. AA merged into chemical groups helps to show patterns that were not as clear when AA were described individually. Note that for each pair of figures (a–i) the y-axis differs, representing the mol% abundance of the chemical grouping (see Fig. 2). For the purpose of this set of figures, negatively charged and neutral polar groups are shown in separate figures. R^2 and p value are shown for each molecular group. A similar plot is shown in the supplementary material for the MB soil fraction, where significant differences over time were absent or weak ($R^2 < 0.10$; Fig. A6)



NMO fractions in a similar way at both locations (Fig. 1). It is unclear whether the differences are due to change in only one fraction or a combination of both, mineral–organic or organic–organic molecular interactions, but building on the findings herein and the literature (Kleber et al. 2007; Philben et al. 2016), both types of molecular interactions are likely to be important determinants of soil organicN composition (Leinemann et al. 2018). The types of AAs that preferentially bind in the MB (His, Arg, Lys, Cys, Met) relative to those in the NMO (Asx, Thr, Ser) fraction provide information on the chemical interactions driving the observed differences. Positively charged AAs, for example, were relatively more common in the MB compared to the NMO fraction, consistent with electrostatic interactions expected to occur between positively charged molecules and negatively charged silica and aluminum dominated minerals (Mikutta et al. 2010). The results are also unique in that Cys and Met were more associated with the MB fraction, suggesting that other mechanisms, perhaps related to Fe and Al crystalline minerals (Rasmussen et al. 2018), are at play.

Specific AA relative abundances, based on multivariate methods, varied between locations, and also shifted in different ways with locations during pedogenesis (Fig. 4). Rather, the chronosequences were more linked to one another when using AA chemical groupings (Fig. 5) than individual AA. These results thus supported the overall hypothesis of similar AA change with pedogenesis at two independent ecosystems, however, differences with pedogenesis were found to be more related to the NMO rather than the MB associated fractions (Supplementary Table A2a,b). Care must be taken in the interpretation of these relationships because the process of fractionation with SPT may change the nature of AA on minerals. Moreover, there is only limited data on the types of changes associated with AA gradients (e.g. soil pH, mineralogy; Jangid et al. 2013; Williams et al. 2013). OM-coated goethite, for example, has been shown to mobilize up to 32% of OM into the soil solution, to be replaced with other DOM, suggesting that MB organic phases can be active in cycling (Leinemann et al. 2018). However minerals may tend to associate with specific types of chemical organic groups that determine mineral–organic interaction (Rasmussen et al. 2018).

Change with pedogenesis were not only impacted by sink (mineral) properties, but likely impacted by biological communities during ecosystem development. So although AA changes with pedogenesis tended to support current thinking about NMO nitrogen accrual in soil and its relation to changes in expected soil chemistry, the results also show the potential for relationships between biological inputs, Fe and Al-bearing minerals and AA change that occurs during pedogenesis.

Patterns of mineral-bound and organic-associated amino acid fractions in soil

The distributions of AA in both NMO and MB soil in Michigan and Haast appeared to reflect, at least partly, specific biological sources. There is no absolute description of expected organism sources and amounts of proteins that would be deposited in soil, and so comparison of organisms to soil composition must be made with caution, but nevertheless, can be potentially useful. Gly, Ala, Asx, and Glx are typically the dominant AAs of organisms (Chen et al. 2013), and account for over 50% of proteinaceous AAs in the chronosequence soils. Broadly, these same AAs have previously been shown to be dominant in soil (Friedel and Scheller 2002; Werdin-Pfisterer et al. 2009) (Tables A2–A3), however, the simplest AAs (Gly and Ala) and some polar AAs (Ser, Thr, and Pro) tended to occur at greater concentrations in soil by up to ~20–40% relative to theoretical biological sources. These results tend to support the idea that AA source affects the proteinaceous AA distribution in soil, however, there are only relatively weak relationships between it and the DNA coding plant proteome (Fig. A3; Table A3; Chen et al. 2013). Stronger correlations between expected bacterial AAs (His and Ala) and those found in soil, however, are supported. There is evidence that plant-derived organic matter, given time, is transformed to living and dead microbial biomass (e.g. proteins) and held in soil by organo-mineral interactions (Bol et al. 2009; Chenu et al. 2018). Discerning why these and other variations occur in soil will be useful for understanding some of the mechanisms of proteinaceous N turnover (Amelung and Zhang 2001; Glaser and Amelung 2002; Vranova et al. 2012), and partitioning into MB and NMO soil fractions.

Eleven of seventeen AAs showed similar enrichment or depletion on MB relative to NMO at both locations. These results suggest that selection mechanisms in addition to biological source, such as those associated with the chemistry of the soil (Tables 1, 2) affect the composition of soil AAs (Dümig et al. 2012). A straightforward mechanism of AA accrual or attachment in soil can occur through electrostatic forces, such as cation exchange (Vieublé Gonod et al. 2006; Rothstein 2010). With the permanent negatively charged minerals, it was expected and data supported that positively charged (high pI; Fig. 3) AAs would be enriched and negatively charged (or low pI) AAs depleted respectively, in the MB compared to the NMO fraction (Fig. 1). Soil are chemically diverse, and so support for this working hypothesis is an important confirmation that electrostatic forces, such as those on mineral surfaces are important for AA and perhaps binding characteristics of electrostatic molecules in soil in situ. The turnover rate of molecules bound to minerals are needed to understand its role in organic C–N accrual in soil.

Amino acids with sulfur side chain groups (Met and Cys) and with amphiphilic sidechain (Tyr and His) were also enriched in MB relative to the NMO fractions in both ecosystems. The role of the sulfur containing AAs in proteins is known to be important in binding to metal ions and redox reactions (reductant) on the active sites of proteins (Betts and Russell 2003; Brosnan and Brosnan 2006), but little is known about their role in supporting the occurrence of proteinaceous AAs in soil organic matter. Similarly, His is commonly found in metal binding motifs. The protons of His can be transferred on and off easily and this is ideal for charge relay systems, such as those found within catalytic triads in proteases. The results support the importance of electrostatic forces in determining the chemistry of soil organic matter, but also suggest that other mechanisms, related to the chemistry of amphiphilic side chains, for example, offer new information useful for understanding organic N accrual in soil.

The enrichment of sulfur and amphiphilic AA in MB relative to NMO fractions could be related to interactions with metal ions acting as interfaces between the AA and the mineral surfaces. His, in addition, is one of three proteinaceous AAs with an aromatic ring, and could be involved in stacking interactions with other aromatic side chains (Betts and

Russell 2003). As weathering progresses, aromatic compounds are thought to bind to mineral surfaces through reactive OH sites associated with short-range order minerals (Kramer et al. 2012). Short-range order minerals are observed along with Fe and Al bearing minerals that indicate progressive soil weathering with ecosystem development. They provide an example of the potential that Fe and Al based minerals bind aromatic moieties in the mineral soil fraction during ecosystem development (Table 3). Hydrophilic neutral (HiN) organic fractions with high nitrogen and acidic conditions can enhance sorption of aromatics (Young et al. 2018), perhaps through metal ion interfaces. The importance that metal ions, stacking interactions, and hydroxyl reactive sites play in binding to soil minerals provide hypotheses about their role in supporting soil organic N molecular composition and accumulation during ecosystem development.

Neutral polar AAs (Asx, Ser and Thr) were more associated with NMO fractions relative to that of the MB soil. This could be explained by two different mechanisms. One is the hydrophilic nature and strong interaction of these AAs with soil NMOs (Rothstein 2009) that can have both polar and non-polar faces and resulting in changing interactions with soil solution (Kyte and Doolittle 1982). Despite extensive particulate organic matter (POM) removal, it cannot be completely ruled out that some aggregate released POM may contribute to this organic pool. Another explanation is related to the selective preservation of these AAs through hydrogen bonds associated with organic aggregates that may restrict their chemical accessibility (Schulten and Schnitzer 1998; Senesi et al. 2009; Ahmed et al. 2015) to microbes. Allard (2006) has shown evidence of increasing neutral polar AAs in lignite deposits where non-mineral OM (e.g. peat) is preserved for very long times (myr), and possibly reflecting organic–organic interactions. This supports a hypothesis that non-charged polar AAs may undergo preservation more through interaction with OM than with soil minerals. This could be corroborated by discerning the age of AAs and their turnover in soil.

Patterns of AA change related to soil age and ecosystem development

A major assumption related to the interpretation of SON change associated with ecosystem development, as with all chronosequence studies, was that measurements from these sites are reflective of the pedogenic scale of interest. The patterns of AA and mineral Fe and Al-minerals show consistency across the chronosequences, and study sites within each location are close to one another (1 km²), which help to keep climatic-weather effects from impacting one age and not the others. It is argued that these two chronosystems reflect broad patterns related to ecosystem development. The changing patterns of proteinaceous AAs, herein, are consistent with the type of change that would be expected over pedogenically relevant timescales (Williams et al. 2013). Previous batch equilibrium studies tested binding of AAs and carboxylic acids to soil minerals (over several days) and have shown the effects of molecular interactions with minerals (Vieublé Gonod et al. 2006; Strahm and Harrison 2008). Field relevant chronosequence based research is limited, but can aid understanding and confirming both MB and NMO fraction changes resulting from pedogenesis (Mikutta et al. 2010). In that particular study, negatively charged AAs were important for binding to the very old and highly weathered soils in Hawaii. Though binding of a different sort was described in our younger chronosequence dominated by changes in positively charged AA, they still are indicative of electrostatic mechanisms following hypothesized trends in a field study.

The results supported the overall hypothesis of similar AA chemical change with pedogenesis at two locations. Though it was expected that the NMO-dominated fraction would shift, the changes with pedogenesis were much more associated with it than the MB fraction (Fig. A6). Care must be taken in the interpretation of these relationships because the process of fractionation with SPT may change the nature of AA on minerals. It is suspected that the changes observed in positively charged AAs are related to Fe and Al mineral changes, however, it could also be the result of interactions with organic dominated fractions. The MB fraction is considered to have greater influence on the persistence of organic matter than non-mineral organic matter (Poirier et al. 2005; Bol et al. 2009) and could thus help to explain its lack of

change with pedogenesis. This would suggest little turnover of AA, however, consistency in this fraction over time could also be related to simple domination of cation exchange mechanisms which continuously select for a new set of chemically similar AA's, despite the potential for some turnover (Turner et al. 2017; Leinemann et al. 2018). Changes in AA groupings in the NMO fractions agree with pedogenic measurements whereby soils are dominated by positive charges during early weathering and ecosystem development (Buol et al. 2011). There is some thought that the Haast system is undergoing retrogression by 6500 years and thus help to explain some increases in negative and decreases in positively-charged AA during the latter developmental stage. Further research into these mechanisms and whether they are affected by methodological challenges associated with extraction of the heavy fraction are needed.

The increase of positively-charged His during pedogenesis were found to occur previously over several hundred years of succession (Werdin-Pfisterer et al. 2009), but these results were based on water extractable AAs, and so it is difficult to compare to the current study. The water soluble fraction was dominated by polar and negatively charged AAs, nevertheless, perhaps a consequence of their high solubility and repulsion from mineral surfaces. This is a logical scenario that support many Haast and WSP findings related to organic–organic and mineral–organic interactions that simultaneously co-occur (Kleber et al. 2007). Increasing positively charged and aromatic AA relative abundances during early ecosystem development are also consistent in this regard. Regardless of the mechanism, consistent patterns related to pedogenesis across two concurrently studied and independent locations support the need for further research into both mineral–organic and organic–organic interactions and the extent of their global implications of organic nitrogen turnover and persistence.

Patterns of AA change associated with biological shifts during pedogenesis

The specific types of change in several chemical AA groups could explain the common trends during pedogenesis across the two sites (Fig. 5). Some of these changes may reflect shifts in vegetation structure (thus contributions to SOM formation), however, there was low evidence for a vegetation effect on soil AA.

However, a model of the way biological changes can exert effects on AA can be demonstrated with bacteria. The soil AA Gly, an important driver of change for the nonpolar AAs, for example, follows a close trend with that of DNA encoding for Gly rich proteins of Actinobacteria (Supplementary Table A.3). Actinobacterial rRNA genes decline from 60 to 35% during ecosystem development and thus help to explain this trend (Williams et al. 2013). Similarly, Acidobacterial DNA which increases 6X during ecosystem development encode for His-rich proteins and help to explain the increasing concentrations of NMO soil His over the many hundreds of years of pedogenesis (Fig. 5). Hence, though chemistry is known to play a role in the soil (sink) determining organic matter composition, the inputs contributed by biological sources, such as AAs from bacteria also determine organic matter chemistry in soil (e.g. Kögel-Knabner et al. 2008). Data herein focus on bacterial contributions to organic N, but as information on fungal phylogenomics increases in databases it soon should be possible to better relate fungal community shifts with organic matter dynamics during pedogenesis.

Glycine and Ala are two of the most abundant AAs, and are also very common AAs in the bacterial cell wall (Koch 2006), but their shifts, as noted above, appear to more associated with the 2X decline in Actinobacteria. Enantiomers of alanine can also serve as indicators of bacterial contributions in soils, and provide a means to further test this hypothesis (Amelung et al. 2008). The proportion of Val is an important driver of change of non-polar AAs, and has been reported to be relatively rich in the extract of bacterial extracellular proteins (Huntjens 1972), which, might reflect a relative decline in contribution of bacterial compared to fungal extracellular proteins to SOM during the latter stages of pedogenesis. It is notable that neutral polar Ser and Thr, which are relatively rich in fungal cell walls (Wagner and Mutatkar 1968), increased during pedogenesis. Fungal total and relative contributions to microbial biomass can help to explain this because fungi generally increase during ecosystem development (Moon 2015), concomitant with changes in soil organic matter (Friedel and Scheller 2002; Rothstein 2009, 2010). Thus, not only the chemistry of the soil sink, but also that of the soil inputs need to be simultaneously

considered to understand mechanisms of soil organic N and organic matter accrual.

Conclusion

There were, as hypothesized, consistent differences in AA composition in MB compared to NMO fractions at two geographically independent and climatically different developmental chronosequences. This result helps to provide evidence for repeatable patterns of soil N accrual across the soil landscape. There is evidence, for example, for the preferential association of basic (electrostatic) and those AA with amphiphilic side chains in the MB relative to the NMO fraction.

Fractionation of AA could be linked to soil mineral effects, however, this study suggested that with soil development, the contribution of NMO-interactions with AAs and proteins are most dynamic, compared to the MB fraction. Change in AAs occurred, however, that were consistent with Fe and Al-mineral changes with pedogenesis, and fit with hypothesized changes in soil electrostatic charge. Though not surprising, the source of the AAs from different types of microbiota could also play a role in the specific AA contributions to organic matter. The role of the soil as a selective force through NMO-AA and mineral-AA interactions are in need of further scrutiny to better understand the mechanisms of proteinaceous AA contributions to soil formation and nutrient turnover. Discerning the underlying principles associated with SOM development have the potential for eventual translation into better descriptions of global C–N cycling, and management of soils for organic matter accrual.

Acknowledgements This research was funded by the United States Department of Agriculture National Institute of Food and Agriculture Foundational Programs (grant# 2011-03815). We acknowledge the DNR of the state of Michigan, Dr. Shankar G. Shanmugam for collecting soil samples from Lake Michigan chronosequence, Dr. Madhavi L. Kakumanu for the density fractionation of soils, Dr. Chao Shang for technical advice on the HPLC instrumentation, and Thurman Haynes for extraction of soil Fe and Al mineral fractions.

References

- Abe T, Watanabe A (2004) X-ray photoelectron spectroscopy of nitrogen functional groups in soil humic acids. *Soil Sci*

- 169:35–43. <https://doi.org/10.1097/01.ss.0000112016.97541.28>
- Ahmed AA, Thiele-Bruhn S, Aziz SG et al (2015) Interaction of polar and nonpolar organic pollutants with soil organic matter: sorption experiments and molecular dynamics simulation. *Sci Tot Environ* 508:276–287
- Allard B (2006) A comparative study on the chemical composition of humic acids from forest soil, agricultural soil and lignite deposit: bound lipid, carbohydrate and amino acid distributions. *Geoderma* 130:77–96. <https://doi.org/10.1016/j.geoderma.2005.01.010>
- Amelung W (2003) Nitrogen biomarkers and their fate in soil. *J Plant Nutr Soil Sci* 166:677–686. <https://doi.org/10.1002/jpln.200321274>
- Amelung W, Zhang X (2001) Determination of amino acid enantiomers in soils. *Soil Biol Biochem* 33:553–562. [https://doi.org/10.1016/S0038-0717\(00\)00195-4](https://doi.org/10.1016/S0038-0717(00)00195-4)
- Amelung W, Brodowski S, Sandhage-Hofmann A, Bol R (2008) Combining biomarker with stable isotope analyses for assessing the transformation and turnover of soil organic matter. Elsevier, San Diego, pp 155–250
- Betts MJ, Russell RB (2003) Amino acid properties and consequences of substitutions. *Bioinform Genet* 317:289
- Bol R, Poirier N, Balesdent J, Gleixner G (2009) Molecular turnover time of soil organic matter in particle-size fractions of an arable soil. *Rapid Commun Mass Spectrom* 23:2551–2558
- Bosch L, Alegría A, Farré R (2006) Application of the 6-aminoquinolyl-*N*-hydroxysuccinimidyl carbamate (AQC) reagent to the RP-HPLC determination of amino acids in infant foods. *J Chromatogr B* 831:176–183. <https://doi.org/10.1016/j.jchromb.2005.12.002>
- Brosnan JT, Brosnan ME (2006) The sulfur-containing amino acids: an overview. *J Nutr* 136:1636S–1640S
- Buol SW, Southard RJ, Graham RC, McDaniel PA (2011) Soil genesis and classification. Wiley, Chichester
- Chen W, Shao Y, Chen F (2013) Evolution of complete proteomes: guanine-cytosine pressure, phylogeny and environmental influences blend the proteomic architecture. *BMC Evol Biol* 13:219
- Chenu C, Angers DA, Barré P et al (2018) Increasing organic stocks in agricultural soils: knowledge gaps and potential innovations. *Soil Tillage Res.* <https://doi.org/10.1016/j.still.2018.04.011>
- DiCosto RJ, Weliky DP, Anderson SJ, Paul EA (2003) ¹⁵N-CPMAS nuclear magnetic resonance spectroscopy and biological stability of soil organic nitrogen in whole soil and particle-size fractions. *Org Geochem* 34:1635–1650. <https://doi.org/10.1016/j.orggeochem.2003.08.005>
- Dümig A, Häusler W, Steffens M, Kögel-Knabner I (2012) Clay fractions from a soil chronosequence after glacier retreat reveal the initial evolution of organo-mineral associations. *Geochim Cosmochim Acta* 85:1–18. <https://doi.org/10.1016/j.gca.2012.01.046>
- Eger A, Almond PC, Condon LM (2011) Pedogenesis, soil mass balance, phosphorus dynamics and vegetation communities across a Holocene soil chronosequence in a super-humid climate, South Westland, New Zealand. *Geoderma* 163:185–196
- Fan T, Lane AN, Chekmenev E et al (2004) Synthesis and physico-chemical properties of peptides in soil humic substances. *J Pept Res* 63:253–264
- Friedel JK, Scheller E (2002) Composition of hydrolysable amino acids in soil organic matter and soil microbial biomass. *Soil Biol Biochem* 34(3):315–325. [https://doi.org/10.1016/S0038-0717\(01\)00185-7](https://doi.org/10.1016/S0038-0717(01)00185-7)
- Gärdenäs AI, Ågren GI, Bird JA et al (2011) Knowledge gaps in soil carbon and nitrogen interactions—from molecular to global scale. *Soil Biol Biochem* 43:702–717. <https://doi.org/10.1016/j.soilbio.2010.04.006>
- Glaser B, Amelung W (2002) Determination of ¹³C natural abundance of amino acid enantiomers in soil: methodological considerations and first results. *Rapid Commun Mass Spectrom* 16:891–898. <https://doi.org/10.1002/rcm.650>
- Grandy AS, Neff JC (2008) Molecular C dynamics downstream: the biochemical decomposition sequence and its impact on soil organic matter structure and function. *Sci Tot Environ* 404:297–307. <https://doi.org/10.1016/j.scitotenv.2007.11.013>
- Hobara S, Osono T, Hirose D et al (2014) The roles of microorganisms in litter decomposition and soil formation. *Biogeochemistry* 118:471–486
- Hou S, He H, Zhang X et al (2009) Determination of soil amino acids by high performance liquid chromatography-electrospray ionization-mass spectrometry derivatized with 6-aminoquinolyl-*N*-hydroxysuccinimidyl carbamate. *Talanta* 80:440–447. <https://doi.org/10.1016/j.talanta.2009.07.013>
- Huntjens JLM (1972) Amino acid composition of humic acid-like polymers produced by streptomycetes and of humic acids from pasture and arable land. *Soil Biol Biochem* 4:339–345. [https://doi.org/10.1016/0038-0717\(72\)90030-2](https://doi.org/10.1016/0038-0717(72)90030-2)
- Jangid K, Whitman WB, Condon LM et al (2013) Progressive and retrogressive ecosystem development coincide with soil bacterial community change in a dune system under lowland temperate rainforest in New Zealand. *Plant Soil* 367(1–2):235–247
- Jaworska H, Dąbkowska-Naskręt H, Kobierski M (2016) Iron oxides as weathering indicator and the origin of Luvisols from the Vistula glaciation region in Poland. *J Soils Sediments* 16:396–404
- Jenkinson DS, Coleman K (2008) The turnover of organic carbon in subsoils. Part 2. Modelling carbon turnover. *Eur J Soil Sci* 59:400–413. <https://doi.org/10.1111/j.1365-2389.2008.01026.x>
- Kleber M, Sollins P, Sutton R (2007) A conceptual model of organo-mineral interactions in soils: self-assembly of organic molecular fragments into zonal structures on mineral surfaces. *Biogeochemistry* 85:9–24. <https://doi.org/10.1007/s10533-007-9103-5>
- Knicker H (2011) Soil organic N - An under-rated player for C sequestration in soils? *Soil Biol Biochem* 43:1118–1129. <https://doi.org/10.1016/j.soilbio.2011.02.020>
- Knicker H, Hatcher PG (1997) Survival of protein in an organic-rich sediment: possible protection by encapsulation in organic matter. *Naturwissenschaften* 84:231–234. <https://doi.org/10.1007/s001140050384>

- Koch AL (2006) *The bacteria: their origin, structure, function and antibiotics*. Springer, Berlin
- Kögel-Knabner I, Guggenberger G, Kleber M, Kandeler E, Kalbitz K, Scheu S, Eusterhues K, Leinweber P (2008) Organo-mineral associations in temperate soils: integrating biology, mineralogy, and organic matter chemistry. *J Plant Nutr Soil Sci* 171(1):61–82
- Kramer MG, Sanderman J, Chadwick OA et al (2012) Long-term carbon storage through retention of dissolved aromatic acids by reactive particles in soil. *Glob Chang Biol* 18:2594–2605
- Kyte J, Doolittle RF (1982) A simple method for displaying the hydrophobic character of a protein. *J Mol Biol* 157:105–132. [https://doi.org/10.1016/0022-2836\(82\)90515-0](https://doi.org/10.1016/0022-2836(82)90515-0)
- Leinemann T, Preusser S, Mikutta R, Kalbitz K et al (2018) Multiple exchange processes on mineral surfaces control the transport of dissolved organic matter through soil profiles. *Soil Biol Biochem* 118:79–90
- Leinweber P, Kruse J, Baum C et al (2013) Advances in understanding organic nitrogen chemistry in soils using state-of-the-art analytical techniques. *Adv Agron* 119:e151
- Lichter J (1995a) Mechanisms of plant succession in coastal Lake Michigan sand dunes. University of Minnesota, Minneapolis
- Lichter J (1995b) Lake Michigan beach-ridge and dune development, lake level, and variability in regional water balance. *Quat Res* 44:181–189
- Lichter J (1998) Rates of weathering and chemical depletion in soils across a chronosequence of Lake Michigan sand dunes. *Geoderma* 85:255–282
- Lowe LE (1973) Amino acid distribution in forest humus layers in British Columbia. *Soil Sci Soc Am J* 37:569–572
- Ma L (2015) Soil organic nitrogen—investigation of soil amino acids and proteinaceous compounds. Doctoral Dissertations
- Marschner B, Brodowski S, Dreves A et al (2008) How relevant is recalcitrance for the stabilization of organic matter in soils? *J Plant Nutr Soil Sci* 171:91–110. <https://doi.org/10.1002/jpln.200700049>
- Meentemeyer V (1978) Macroclimate and lignin control of litter decomposition rates. *Ecology* 59:465–472. <https://doi.org/10.2307/1936576>
- Mikutta R, Kaiser K, Dörr N et al (2010) Mineralogical impact on organic nitrogen across a long-term soil chronosequence (0.3–4100 kyr). *Geochim Cosmochim Acta* 74:2142–2164. <https://doi.org/10.1016/j.gca.2010.01.006>
- Moon J (2015) Selective accrual and dynamics of proteinaceous compounds during pedogenesis: testing source and sink selection hypotheses. Virginia Tech, Blacksburg
- Moon J, Ma L, Xia K, Williams MA (2016) Plant–Microbial and mineral contributions to amino acid and protein organic matter accumulation during 4000 years of pedogenesis. *Soil Biol Biochem* 100:42–50. <https://doi.org/10.1016/j.soilbio.2016.05.011>
- Palmer RWP, Doyle RB, Grealish GJ, Almond PC (1985) Soil studies in South Westland 1984/1985. Soil Bureau District Office Report NP 2. Department of Scientific and Industrial Research, New Zealand
- Parton WJ, Ojima DS, Schimel DS, Kittel TGF (1992) Development of simplified ecosystem models for applications in Earth system studies: The Century experience. In: Ojima DS (ed) *Modeling the earth system*. Proceedings from the 1990 Global Change Institute on Earth System Modeling, 16–27 July 1990. Aspen Global Change Institute, Aspen
- Philben M, Ziegler SE, Edwards KA et al (2016) Soil organic nitrogen cycling increases with temperature and precipitation along a boreal forest latitudinal transect. *Biogeochemistry* 127:397–410. <https://doi.org/10.1007/s10533-016-0187-7>
- Rasmussen C, Heckman K, Wieder WR, Keiluweit M et al (2018) Beyond clay: towards an improved set of variables for predicting soil organic matter content. *Biogeochemistry* 137(3):297–306
- Poirier N, Sohi SP, Gaunt JL, Mahieu N, Randall EW, Powlson DS, Evershed RP (2005) The chemical composition of measurable soil organic matter pools. *Org Geochem* 36(8):1174–1189
- Rattenbury MS, Jongens R, Cox SC (2010) *Geology of the Haast Area*. Institute of Geological & Nuclear Sciences 1: 250,000 Geological Map 14. GNS Science Lower Hutt
- Rothstein DE (2009) Soil amino-acid availability across a temperate-forest fertility gradient. *Biogeochemistry* 92:201–215
- Rothstein DE (2010) Effects of amino-acid chemistry and soil properties on the behavior of free amino acids in acidic forest soils. *Soil Biol Biochem* 42:1743–1750. <https://doi.org/10.1016/j.soilbio.2010.06.011>
- Rovira P, Fernández P, Coûteaux M, Ramón VV (2005) Changes in the amino acid composition of decomposing plant materials in soil: species and depth effects. *Commun Soil Sci Plant Anal* 36:2933–2950. <https://doi.org/10.1080/00103620500306122>
- Rovira P, Kurz-Besson C, Hernández P et al (2008) Searching for an indicator of N evolution during organic matter decomposition based on amino acids behaviour: a study on litter layers of pine forests. *Plant Soil* 307:149–166. <https://doi.org/10.1007/s11104-008-9592-6>
- Schmidt MWI, Torn MS, Abiven S et al (2011) Persistence of soil organic matter as an ecosystem property. *Nature* 478:49–56
- Schulten H-R, Schnitzer M (1998) The chemistry of soil organic nitrogen: a review. *Biol Fertil Soils* 26:1–15. <https://doi.org/10.1007/s003740050335>
- Senesi N, Xing B, Huang PM (2009) Biophysico-chemical processes involving natural nonliving organic matter in environmental systems. Wiley, Hoboken
- Sollins P, Swanston C, Kleber M et al (2006) Organic C and N stabilization in a forest soil: evidence from sequential density fractionation. *Soil Biol Biochem* 38:3313–3324. <https://doi.org/10.1016/j.soilbio.2006.04.014>
- Stevenson FJ (1982) Organic forms of soil nitrogen. In: Stevenson FJ (ed) *Nitrogen in agricultural soils*. American Society of Agronomy, Madison, pp 101–104
- Strahm BD, Harrison RB (2008) Controls on the sorption, desorption and mineralization of low-molecular-weight organic acids in variable-charge soils. *Soil Sci Soc Am J* 72:1653. <https://doi.org/10.2136/sssaj2007.0318>
- Turner S, Meyer-Stüve S, Schippers A, Guggenberger G, Schaarschmidt F, Wild B, Richter A, Dohrmann R, Mikutta R (2017) Microbial utilization of mineral-associated nitrogen in soils. *Soil Biol Biochem* 104:185–196

- Turner BL, Wells A, Andersen KM, Condron LM (2012) Patterns of tree community composition along a coastal dune chronosequence in lowland temperate rain forest in New Zealand. *Plant Ecol* 213:1525–1541. <https://doi.org/10.1007/s11258-012-0108-3>
- Vieublé Gonod L, Jones DL, Chenu C (2006) Sorption regulates the fate of the amino acids lysine and leucine in soil aggregates. *Eur J Soil Sci* 57:320–329. <https://doi.org/10.1111/j.1365-2389.2005.00744.x>
- Vranova V, Zahradnickova H, Janous D et al (2012) The significance of D-amino acids in soil, fate and utilization by microbes and plants: review and identification of knowledge gaps. *Plant Soil* 354:21–39. <https://doi.org/10.1007/s11104-011-1059-5>
- Wagner GH, Mutatkar VK (1968) Amino components of soil organic matter formed during humification of ¹⁴C Glucose I. *Soil Sci Soc Am J* 32:683. <https://doi.org/10.2136/sssaj1968.03615995003200050030x>
- Werden-Pfisterer NR, Kielland K, Boone RD (2009) Soil amino acid composition across a boreal forest successional sequence. *Soil Biol Biochem* 41:1210–1220. <https://doi.org/10.1016/j.soilbio.2009.03.001>
- Williams MA, Jangid K, Shanmugam SG, Whitman WB (2013) Bacterial communities in soil mimic patterns of vegetative succession and ecosystem climax but are resilient to change between seasons. *Soil Biol Biochem* 57:749. <https://doi.org/10.1016/j.soilbio.2012.08.023>
- Young RB, Avneri-Katz S, McKenna AM et al (2018) Composition-dependent sorptive fractionation of anthropogenic dissolved organic matter by Fe(III)-montmorillonite. *Soil Systems* 2(1):14
- Zang X, van Heemst JDH, Dria KJ, Hatcher PG (2000) Encapsulation of protein in humic acid from a histosol as an explanation for the occurrence of organic nitrogen in soil and sediment. *Org Geochem* 31:679–695. [https://doi.org/10.1016/S0146-6380\(00\)00040-1](https://doi.org/10.1016/S0146-6380(00)00040-1)